A Role for the E-Cadherin Cell-Cell Adhesion Molecule during Tumor Progression of Mouse Epidermal Carcinogenesis

Pilar Navarro,* Manuel Gómez,* Angel Pizarro,‡ Carlos Gamallo,§ Miguel Quintanilla,* and Amparo Cano*

*Instituto de Investigaciones Biomédicas, Consejo Superior de Investigaciones Científicas, Departamento de Bioquímica, Facultad Medicina, Universidad Autónoma de Madrid 28029 Madrid, Spain; ‡Servicio de Dermatología, Hospital La Paz, Madrid, Spain; and §Servicio de Anatomía Patológica, Hospital La Paz, Facultad Medicina, Universidad Autónoma de Madrid, Madrid, Spain

Abstract. The expression of the cell–cell adhesion molecules E- and P-cadherin has been analyzed in seven mouse epidermal keratinocyte cell lines representative of different stages of epidermal carcinogenesis. An inverse correlation between the amount of E-cadherin protein and tumorigenicity of the cell lines has been found, together with a complete absence of E-cadherin protein and mRNA expression in three carcinoma cell lines (the epithelioid HaCa4 and the fibroblastoid CarB and CarC cells). A similar result has been detected in tumors induced in nude mice by the cell lines, where induction of E-cadherin expression takes place in moderately differentiated squamous cell carcinomas induced by HaCa4 cells, although at much lower levels than in well-differentiated tumors induced by the epithelial PDV or PDVC57 cell lines. Complete absence of E-cadherin expression has been observed in spindle cell carcinomas induced by CarB or CarC cells. P-cadherin protein was detected in all cell lines that exhibit an epithelial (MCA3D, AT5, PDV, and PDVC57) or epithelioid (HaCa4) morphology, as well as in nude mouse tumors, independent of their tumorigenic capabilities. However, complete absence of P-cadherin was observed in the fibroblast-like cells (CarB and CarC) and in spindle cell carcinomas. The introduction of an exogenous E-cadherin cDNA into HaCa4 cells, or reactivation of the endogenous E-cadherin gene, leads to a partial suppression of the tumorigenicity of this highly malignant cell line. These results suggest a role for E-cadherin in the progression to malignancy of mouse epidermal carcinogenesis. They also suggest that the loss of both E- and P-cadherin could be associated to the final stage of carcinogenesis, the development of spindle cell carcinomas.

CELL adhesion mechanisms play a major role in vital processes such as embryogenesis, tissue and organ pattern formation and maintenance of specific tissue architecture (Edelman, 1985; Thiery et al., 1982). Calcium-dependent cell–cell adhesion molecules are one of the major components involved in the various processes of intercellular adhesion (Takeichi et al., 1985). In vertebrates, calcium-dependent cell–cell adhesion molecules identified so far constitute a family of transmembrane glycoproteins, of 119–135 kD, for which the general term cadherins has been proposed (see Takeichi, 1988, 1990 for reviews).

The different members of the family, identified in various tissues and species, can be grouped in three distinct categories, exemplified in the mouse by (a) N-cadherin (Hatta and Takeichi, 1986; Hatta et al., 1985), present mostly in neural tissues; (b) E-cadherin (identical to uvomorulin) (Yoshida-Noro et al., 1984; Hyafil et al., 1980; Peyrieras et al., 1985), expressed in epithelial tissues; and (c) P-cadherin, present both in epithelial and nonepithelial tissues with major prevalence at the placenta (Nose and Takeichi, 1986). All members of the family present strong homology at the amino acid

level (Nose et al., 1987; Hatta et al., 1988; Ringwald et al., 1987), but distinct immunological properties and binding specificities (Nose et al., 1988; Miyatani et al., 1989). The pattern of expression and binding specificities of the different subfamilies are consistent with the proposed role of these molecules in the segregation of differentiating tissues during embryogenesis and in the morphogenetic processes involved in the generation of an organism (Takeichi, 1988, 1990, 1991).

During tumorigenesis, profound alterations in intercellular and cell-to-substratum interactions take place (for reviews, see Hynes, 1989; Parish et al., 1987). Such alterations are particularly evident in tumorigenesis of epithelial tissues, where the malignant cells have to pass through the basement membrane barrier in order to invade and metastasize other tissues. Even before invading adjacent tissues, the malignant cells loosen their adhesion to their original neighbors. The molecular mechanisms underlying such alterations are largely unknown and only recently have begun to be investigated. Among them, changes in cell–cell interactions mediated by the cadherin family of molecules in rela-

tion to malignancy have received increasing interest in the last few years. Studies on tissue sections of various human carcinomas have shown that E-cadherin is expressed in both differentiated and dedifferentiated tumors (Eidelman et al., 1989; Shimoyama et al., 1989), although lower levels appear to be present in poorly differentiated carcinomas (Shimoyama et al., 1989). A recent study on E-cadherin expression in several human carcinoma cell lines indicates that acquisition of the invasion properties of dedifferentiated fibroblastoid carcinoma cells is associated with the loss of E-cadherin expression (Frixen et al., 1991). These observations, together with previous similar results with H-ras-transformed MDCK cells (Behrens et al., 1989), support a role for E-cadherin as an antiinvasive molecule, and as a marker of the differentiation grade of epithelial carcinomas (Frixen et al., 1991). The expression of P-cadherin has so far only been reported in one study of human epithelial carcinomas (Shimoyama et al., 1989).

Our laboratory is investigating the role of E- and P-cadherin during the tumorigenic process of mouse epidermal carcinogenesis. Both cadherins are the only members of the calcium dependent cell-cell adhesion molecules expressed in normal mouse skin with P-cadherin restricted to the proliferative basal layer and E-cadherin expressed in the basal and suprabasal layers (Nose and Takeichi, 1986). The model of two-stage mouse skin carcinogenesis is based in the progressive induction of premalignant papillomas and invasive carcinomas by treatment with initiating and promoting chemical agents (Boutwell, 1974; Hecker, 1978; Hennings et al., 1985). A variety of cell lines can be derived from tumors and by in vitro transformation of primary epidermal cells, providing the opportunity of an in vitro approach to the mouse skin carcinogenesis system (for review, see Balmain and Brown, 1988).

In this study, we have analyzed the expression of P- and E-cadherin in seven mouse epidermal keratinocyte cell lines, ranging from immortalized nontumorigenic to highly malignant carcinoma-derived cells, which express morphological phenotypes in culture of epithelial, epithelioid or fibroblastoid cells. All cell lines used in this study have been previously characterized in regard to their expression of normal and mutant H-ras alleles (Quintanilla et al., 1986, 1991) and to their differentiation pattern in relation to cytokeratin expression (Díaz-Guerra, M., C. Bauluz, S. Haddow, J. L. Jorcano, A. Cano, A. Balmain, and M. Quintanilla, manuscript submitted for publication). An inverse correlation between the amount of E-cadherin protein present and the tumorigenicity of the different cell lines has been found. This correlation has been detected both in cell cultures and in tumors induced by injection of the cell lines in nude mice. Complete absence of both E- and P-cadherin has been detected in cells and tumors of two spindle carcinoma fibroblastoid cell lines, whereas P-cadherin, but not E-cadherin, was present in a squamous cell carcinoma line. Furthermore, we show that a partial suppression of the tumorigenicity can be obtained by transfection of E-cadherin cDNA into this latter, highly malignant epithelioid carcinoma cell line. Our results suggest that, in mouse epidermal carcinogenesis, the progressive loss of E-cadherin can contribute to the malignancy of squamous cell carcinomas. On the other hand, the complete loss of both E- and P-cadherin could also play a

role in the further progression towards poorly differentiated spindle cell carcinomas.

Materials and Methods

Cell Lines and Growth Conditions

The origin of the mouse epidermal keratinocyte cell lines used in the present study (MCA3D, AT5, PDV, PDVC57, HaCa4, CarB and CarC) is described elsewhere (Díaz-Guerra, M., C. Bauluz, S. Haddow, J. L. Jorcano, A. Cano, A. Balmain, and M. Quintanilla, manuscript submitted for publication) and is briefly summarized in Table I. All of the epidermal cell lines were grown in HAM F-12 medium supplemented with a complete set of amino acids (Gibco Ltd., Paisley, Scotland), 5 or 10% FCS and the antibiotics amphotericin B (2.5 μg/ml), ampicillin (100 μg/ml), and gentamicin (32 μg/ml) (Sigma Chemical Co., St. Louis, MO). Mouse 10T1/2 fibroblasts were cultured in Dulbecco's MEM supplemented with 10% FCS and antibiotics. Cells were grown at 37°C in a humidified 5% CO_2 atmosphere.

Transfection Procedure

HaCa4 cells were cotransfected with the pBATEM-2 (Nose et al., 1988) and the pSV2neo vectors (Southern and Berg, 1982) by the calcium-phosphate coprecipitation method essentially as described by Nose et al. (1988). Transfection with 1 μg of pBATEM-2 and 0.1 μg of pSV2neo was carried out in Dulbecco's MEM supplemented with 10% FCS. After 18 h, the DNA-containing medium was replaced by fresh HAM F-12 containing 10% FCS, and 24 h later selection with 0.4 mg/ml G418 (Gibco Ltd.) was begun. Resistant colonies were isolated and tested for E-cadherin expression by immunofluorescence staining and Western immunoblotting. Positive cells were subcloned and used for further studies. The pBATEM-2 vector was kindly provided by M Takeichi (University of Kyoto, Kyoto, Japan), and the pSV2neo vector by J. L. Jorcano (CIEMAT, Madrid, Spain).

Tumorigenicity Assays in Nude Mice

For the tumorigenicity test, cells were collected and washed in PBS and subcutaneously injected in male nu/nu mice, 8–10 wk old. 1 × 10⁶ cells were used for a single injection. In different experiments, mice were either individually injected with the same cell line at three different sites (the two flanks and the neck) or double injected with distinct cells on the left and right flanks. Animals were observed for tumor formation and sacrificed when tumors reached a size of ∼2 cm.

Immunostaining and Histological Procedures

For immunofluorescent staining, cells were grown to confluence on glass coverslips and, after washing in PBS containing 2.5 mM $CaCl_2$ (or 2 mM EGTA), were fixed and permeabilized by the methanol-acetone method. Coverslips were incubated with the mAb ECCD-2 (1/500) or PCD-1 (1/20) as described (Shirayoshi, 1986; Nose and Takeichi, 1986). Goat anti-rat IgG coupled to rhodamine or fluorescein compounds (Nordic Immunologicals Lab., Tilburg, The Netherlands) were used as second antibodies.

Immunocytochemical staining of tumors with the mAb ECCD-2 (1/250) and PCD-1(1/20) was carried out on frozen tissue. Fresh surgically excised tumors were embedded in OCT compound, frozen in liquid nitrogen, and stored at −70°C. Cryostat sections of 5–6 μm were immunostained by the alkaline phosphatase method using biotinylated sheep anti-rat Ig (1/200, Amersham International, Amersham, England) and extravidin-alkaline phosphatase complex (1/250, BioMakor, Rehovot, Israel). The alkaline phosphatase activity was developed using naphtyl ASMX phosphate as substrate and Fast-Red as the chromogen group (Sigma Chemical Co.). As negative control, we used rat anti-mouse Ig as the primary antibody. Immunocytochemical staining of normal mouse skin showing the specific staining pattern of both antibodies was used as positive control.

Dilutions of anti-cadherin antibodies were made in 150 mM NaCl, 10 mM Hepes, pH 7.4, 10 mM $CaCl_2$ (HMF-Ca buffer), containing 1% (wt/vol) BSA and secondary antibodies in PBS containing preimmune goat serum (1:50 dilution). The mAb ECCD2 and PCD-1 were a generous gift of M. Takeichi.

Histological analysis of tumors was carried out on 5–6-μm sections of paraffin embedded material.

Table I. Relationship between E- and P-cadherin Levels and Tumorigenicity of Mouse Epidermal Cells in Nude Mice

Cell lines	Morphology*	Origin	E-cadherin[‡] levels	P-cadherin[§] levels	Relative[‖] tumorigenicity
MCA3D	Ep	Immortalized mouse keratinocytes	100	30	−
AT5	Ep	MCA3D + Human ras	75	56	±
PDV	Ep	Transformed with DMBA in vitro	30[¶]	100	+ +
PDVC57	Ep	Derived from PDV by transplantation	15[¶]	10	+ + +
HaCa4	E	HaMSV/TPA carcinoma	0	82	+ + + +
CarB	F	DMBA/TPA carcinoma	0	0	+ + + +
CarC	F	DMBA/TPA carcinoma	0	0	+ + + +

* Morphology of the cell lines in culture indicated as: Ep, epithelial; E; epithelioid; and F, fibroblastoid.

‡ Levels of E-cadherin detected in whole cell extracts, quantified from densitometric scans of three different autoradiograms such as that shown in Fig. 4 B, are indicated as the percentage of the level detected in MCA3D extracts.

§ Levels of P-cadherin in whole cell extracts, quantified from the densitometric scan of the autoradiogram shown in Fig. 4 C, are indicated as the percentage of the level detected in PDV extracts.

‖ Relative tumorigenicity, indicated as increasing + symbols, was estimated as a function of the latency period to obtain tumors of 1 cm diameter and of the number of tumors induced per injection site. −, no tumors; ±, one tumor in three injection sites with a latency period of 3 mo; + + to + + + +, tumors at all injection sites with latency periods of: + +, 3 wk, + + +, 2 wk, and + + + +, 7-9 d. More details of tumorigenicity of the cell lines are given in Quintanilla et al., 1991, and in Díaz-Guerra, M., C. Bauluz, S. Haddow, J. L. Jorcano, A. Cano, A. Balmain, and M. Quintanilla, manuscript submitted for publication.

¶ The levels of E-cadherin in PDV and PDVC57 whole cell extracts varied between 15 and 50% and 10 and 20%, respectively, of the level detected in MCD3D extracts in the different experiments.

Preparation of Cell Extracts and Western Blotting

Whole-cell extracts, without trypsin treatment, were obtained as follows. Cells grown to confluence on P-100 dishes were washed twice with HMF-Ca buffer and lysed in 0.5 ml lysis buffer (100 mM NaCl, 50 mM Tris-HCl, pH 7.4, 5 mM MgCl₂, 1% Triton X-100, 0.1% SDS, 0.5% Na-deoxycholate, 0.05% NaN₃) containing 10 mM CaCl₂ and a mixture of protease inhibitors (2 mM PMSF, 2 mM iodoacetic acid, 2 mM N-ethylmaleimide, and 1% trasylol; Sigma Chemical Co.). After centrifugation, supernatants were collected, adjusted to 1× Laemmli sample buffer and fractionated on 10% PAGE-SDS gels, as described (Laemmli, 1970).

Trypsin treatment of cells, in the presence of 2.5 mM CaCl₂ or 2 mM EGTA, was carried out as described (Yoshida-Noro et al., 1984). Cell pellets were then resuspended in 100 μl lysis buffer containing 2.5 mM CaCl₂ and the mixture of protease inhibitors and treated as described above.

Western blot analyses of the various cell extracts were carried out essentially as described (Towbin et al., 1979). Samples containing identical amounts of total proteins were run on 10% PAGE-SDS gels and transferred to nitrocellulose paper. After staining with Ponceau Red, the filters were immunoblotted with the mAb ECCD-2 or PCD-1 as described previously (Nose and Takeichi, 1986).

Northern and Southern Blot Analyses

Total RNA from the different cell lines were isolated by the guanidium-thiocyanate procedure (Chomczynski and Sacchi, 1987). Denatured RNA (10 μg) from each sample were fractionated on 1% agarose gels using formaldehyde-phosphate buffer (Rave et al., 1979) and transferred to nylon membranes (Zeta Probe; BioRad, Madrid, Spain) using 10× SSC as described (Maniatis et al., 1982). Hybridization to ³²P-labeled probes was carried out in 4× SSC, 5 mM EDTA, 20 mM H₂NaPO₄, pH 7.0, 1% SDS, 10× Denhardt's solution containing denatured salmon sperm DNA (200 μg/ml) for 20 h at 65°C. Filters were then washed twice in 2× SSC, 0.1% SDS at 65°C for 10 min and twice in 0.1× SSC, 0.1% SDS at 65°C for 20 min. After hybridization to the E-cadherin cDNA probe, the filters were rehybridized with the β-actin cDNA probe in the same conditions.

DNA from the different cell lines was obtained by conventional methods (Maniatis et al., 1982). 10 μg of each DNA sample were digested with BamHI or EcoRI restriction enzymes (Boehringer Mannheim S.A., Barcelona, Spain) and fractionated on 0.7% agarose gels. After blotting to nylon membranes, hybridization to the ³²P-labeled E-cadherin cDNA probe was performed in a solution of 5× SSPE, 50 mM H₂NaPO₄, pH 7.4, 10 mM

sodium pyrophosphate, 0.1% SDS, 2× Denhardt's solution, containing denatured salmon sperm DNA (200 μg/ml) for 20 h at 65°C. Filters were washed in 2× SSPE, 0.1% SDS for 10 min at room temperature, followed by 30 min at 65°C in the same buffer (1× SSPE: 180 mM NaCl, 10 mM H₂NaPO₄, 1 mM EDTA, pH 7.0).

The probe used for E-cadherin detection was the 0.9-kb BamHI fragment cut from the pBATEM-2 plasmid, containing coding sequences from nucleotides 993 to 1920 (Nagafuchi et al., 1987); and for β-actin, a 0.6-kb EcoRI-HindIII fragment of rat β-actin cDNA kindly provided by J. G. Castaño (Department of Biochemistry, Universidad Autónoma de Madrid, Madrid, Spain). Inserts were isolated from plasmids by electrophoresis in agarose, purified by a Geneclean kit (Bio 101 Inc., La Jolla, CA) and labeled by the random primer method (Feinberg and Vogelstein, 1983).

Results

Identification of E- and P-Cadherin in Mouse Epidermal Keratinocytes

The mAbs ECCD-2 and PCD-1 have been shown to recognize mouse E- and P-cadherin, respectively (Shirayoshi et al., 1986; Nose and Takeichi, 1986). Using these antibodies, we have studied the expression of both proteins in seven mouse epidermal keratinocyte cell lines. These include immortalized nontumorigenic keratinocytes (MCA3D, Kulesz-Martin et al., 1983), a cell line derived by transfection of the human T24 H-ras oncogene into MCA3D cell (AT5) (Quintanilla et al., 1991), transformed keratinocytes obtained by treatment of primary epidermal cells with the carcinogen DMBA (PDV and PDVC57; Bremner and Balmain, 1990; Quintanilla et al., 1991) and cell lines derived from carcinomas induced in vivo by the HaMSV retrovirus and TPA (HaCa4; Brown et al., 1986) or by DMBA/TPA treatment (CarB and CarC; Quintanilla et al., 1986).

The cell lines were selected for this study because of their different tumorigenic capabilities in nude mice, ranging from non-tumorigenic to highly malignant (see Table I), and
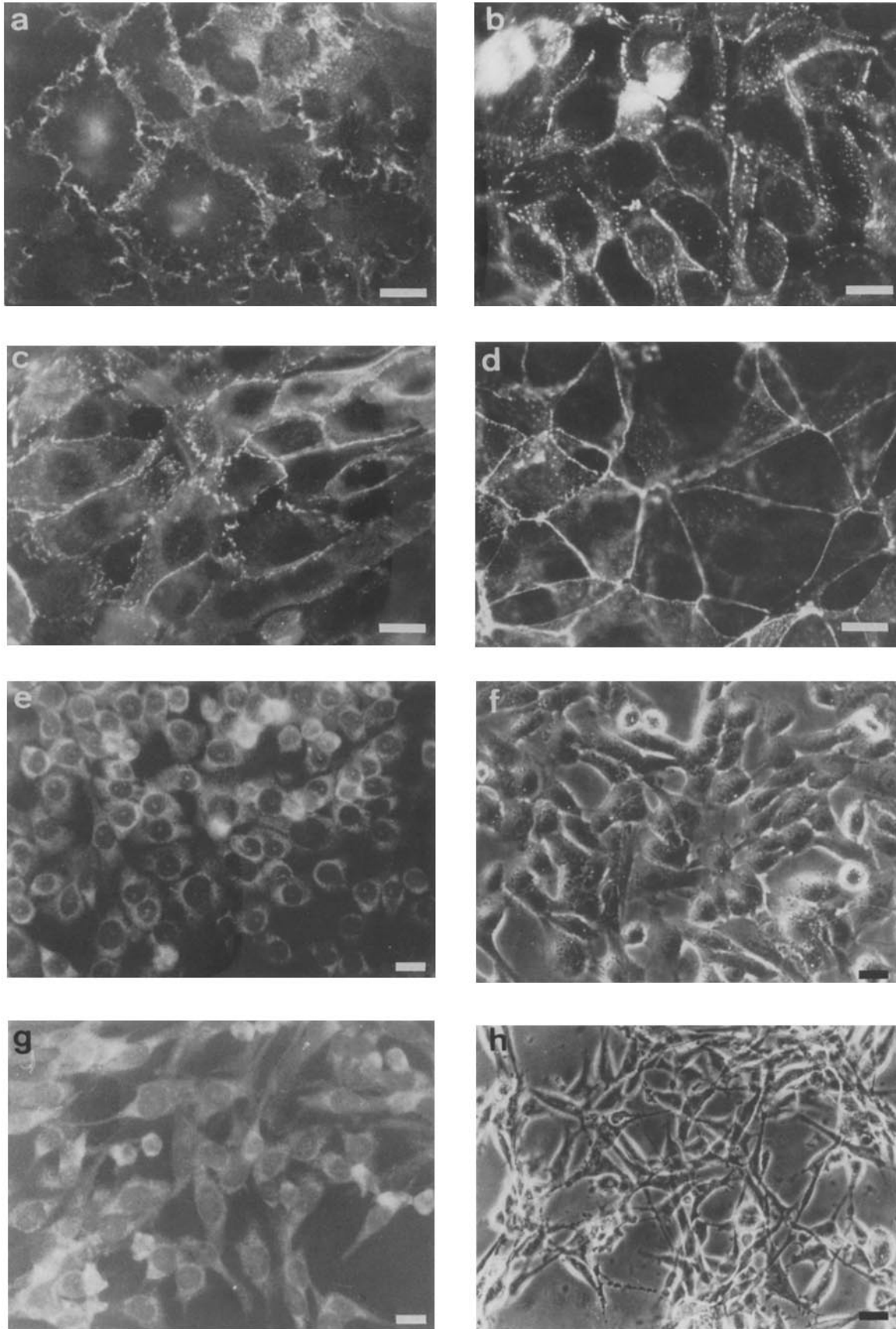
Figure 1. Immunofluorescent staining of epidermal keratinocyte cell lines with the mAb ECCD-2. The different cell lines were grown to confluence on glass coverslips and washed in PBS containing 2.5 mM CaCl$_2$ before and after fixation. Cell lines: (*a*) MCA3D, (*b*) AT5, (*c*) PDV, (*d*) PDVC57, (*e* and *f*) HaCa4, (*g* and *h*) CarB. (*f* and *h*) Phase-contrast images of Haca4 and CarB cells, respectively. Neither the epithelioid HaCa4 nor the fibroblastoid CarB cell lines are specifically stained by the anti–E-cadherin antibody. Bar, 30 μm.
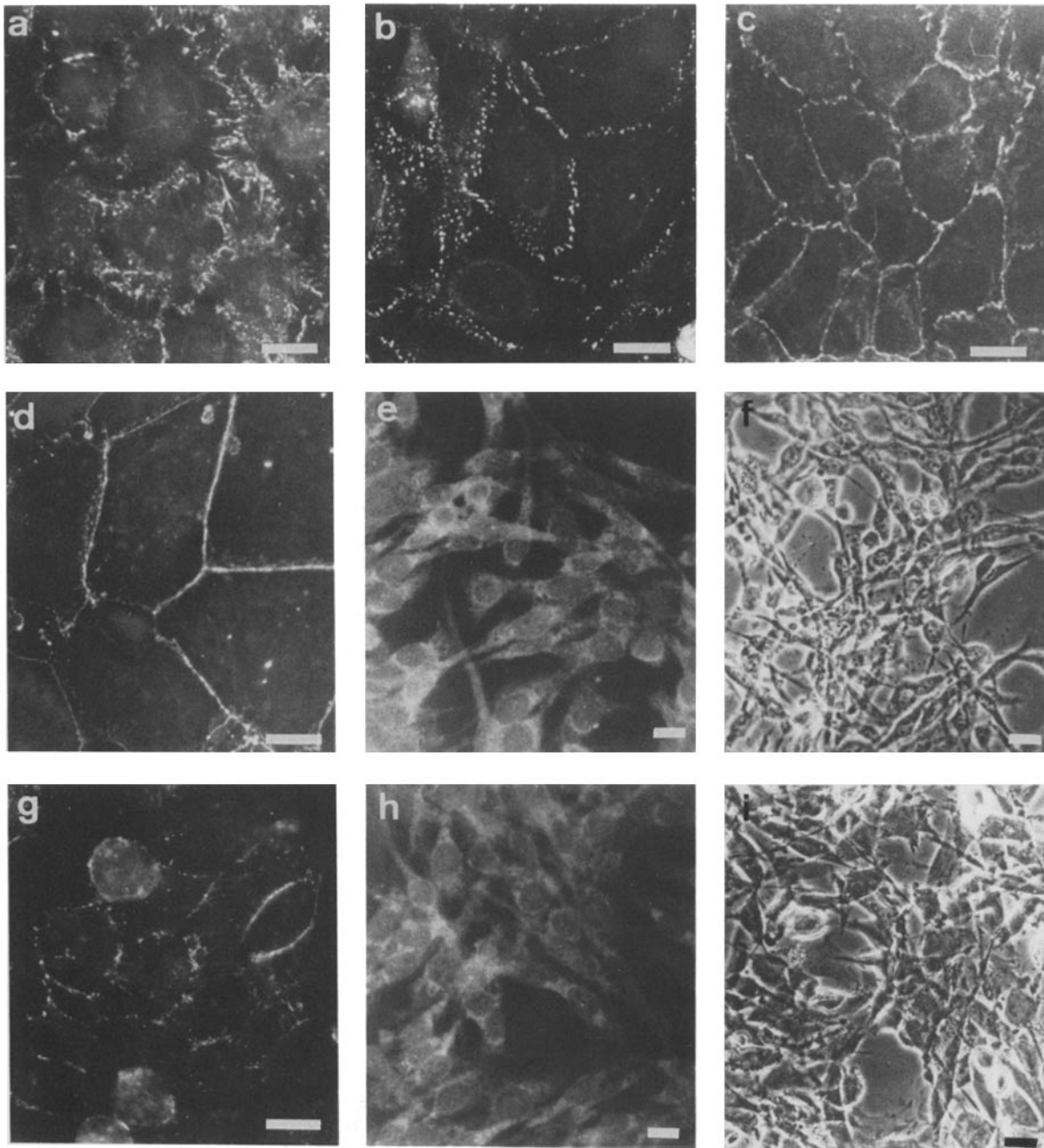
Figure 2. Immunofluorescent staining of epidermal keratinocyte cell lines with the monoclonal antibody PCD-1. Cells were grown to confluence on glass coverslips and washed in PBS containing 2.5 mM CaCl₂ before and after fixation. Cell lines: (*a–d*) as in Fig. 1; (*e* and *f*) CarB; (*g*) HaCa4; (*h* and *i*) CarC. *f* and *i* show phase-contrast images of CarB and CarC cells, respectively. See the positive staining by PCD-1 mAb at the cell–cell interfaces in HaCa4 cells (*g*), in contrast to the negative staining by ECCD-2 mAb in this cell line (compare with Fig. 1 *e*). Bar, 30 μm.

because they exhibit different morphological phenotypes in culture. MCA3D, AT5, PDV, and PDVC57 cells present a typical epithelial morphology with a cobblestone pattern of growth; the HaCa4 cell line, derived from a squamous cell carcinoma, shows an epithelioid phenotype with cell-cell contacts observed only at high density culture conditions (Fig. 1*f*) and CarB and CarC cells, derived from two independent poorly differentiated spindle cell carcinomas, have a fibroblastoid shape (Fig. 1 *h* and Fig. 2, *f* and *i*).

The immunofluorescent staining of the cells with the mAb ECCD-2 showed that the four epithelial cell lines, MCA3D, AT5, PDV, and PDVC57, were stained at the cell–cell contact

regions (Fig. 1, *a–d*). However, both the epithelioid HaCa4 and the fibroblastoid CarB cell line did not show any specific fluorescence with this mAb (Fig. 1, *e* and *g*, respectively). Similar negative staining was also observed in CarC cells (not shown). On the other hand, immunofluorescent staining with the mAb PCD-1 showed that CarB and CarC cells were negative (Fig. 2, *e* and *h*), whereas all the others, including HaCa4, were positive (Fig. 2, *a–d* and *g*).

The antigens recognized by the mAb ECCD-2 and PCD-1 in the epidermal keratinocytes were identified as E- and P-cadherin, respectively, by several criteria. First, localization of the immunofluorescent staining at the cell–cell in-
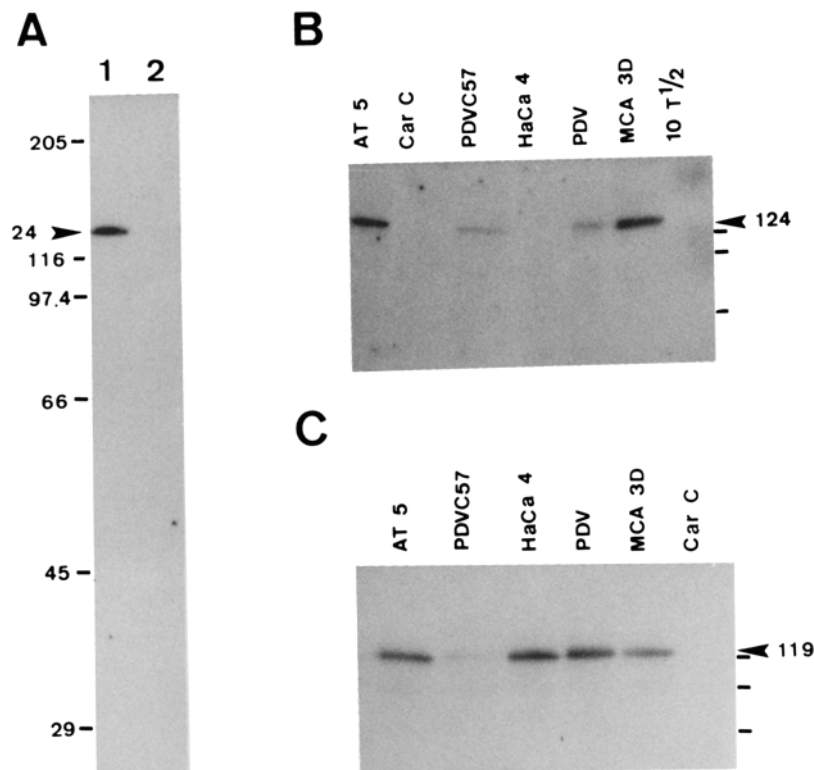
Figure 3. Immunoblot detection of ECCD-2 and PCD-1 antigens in mouse epidermal cells. (*A*) AT5 cells were trypsinized in the presence of 2.5 mM CaCl₂ (lane *1*) or in the presence of 2 mM EGTA (lane *2*) before harvesting and lysis. (*B* and *C*) Whole cell extracts of the various cell lines were obtained from confluent cell monolayers, without trypsinization, and in the presence of 10 mM CaCl₂ and protease inhibitors. Cell lysates were loaded on 10% PAGE-SDS gels at 50 μg protein/lane, transferred to nitrocellulose membranes, and detected with ECCD-2 (*A* and *B*) or PCD-1 (*C*) mAbs. In *A*, migration of the molecular mass markers, in kilodaltons, is indicated on the left. In *B* and *C*, only the significant portion of the gels is shown; migration of the molecular mass markers, 116, 97.4, and 66 kD is indicated by small marks on the right. The estimated molecular mass, in kilodaltons, of the antigens detected by both antibodies is indicated in each panel by arrowheads.

terfaces was dependent on the existence of established intercellular contacts. The immunofluorescence at the cell boundaries was observed only in confluent cells (Fig. 1, *a–d*, and Fig. 2, *a–d* and *g*) or within small colonies in low density cultures, but was absent at the limits of the islands where there are no neighboring cells (not shown). Second, Western blotting of cell extracts obtained in the presence of calcium detected one ECCD-2 immunoreactive polypeptide of 124 kD (Fig. 3 *A*, lane *1*, see also Fig. 3 *B*), and one PCD-1 immunoreactive polypeptide of 119 kD (Fig. 3 *C*), in agreement with the sizes previously reported for mouse E- and P-cadherins, respectively (Yoshida-Noro et al., 1984; Hirano et al., 1987; Nose and Takeichi, 1986). And finally, both polypeptides disappeared when the cells were trypsinized in the presence of EGTA (see in Fig. 3 *A*, lane *2*, one example for ECCD-2 detection); accordingly, the immunofluorescent staining disappeared when the cells were pretreated with EGTA before fixation (not shown).

The Amount of Soluble E-Cadherin Inversely Correlates with Tumorigenicity of the Epidermal Cell Lines

The levels of E- and P-cadherin protein expression were analyzed in whole cell extracts obtained by solubilization of confluent cell monolayers in the presence of calcium and protease inhibitors, as described in Materials and Methods. Aliquots of each cell extract, containing identical amounts of total protein, were loaded onto gels and blotted with ECCD-2 or PCD-1 mAb. The results of a representative experiment are presented in Fig. 3, *B* and *C*. Table I shows a quantitative determination of soluble E- and P-cadherin levels compared to the tumorigenic capabilities of the cell lines after injection in nude mice. As can be observed, an inverse

correlation between the amount of solubilized E-cadherin and tumorigenicity was found. MCA3D and AT5 cells, which are nontumorigenic and weakly tumorigenic, respectively, contained the highest levels of E-cadherin. The protein decreased in the moderately tumorigenic PDV and PDVC57 cell lines and was completely absent in the highly malignant carcinoma derived cells HaCa4, CarC (Fig. 3 *B*, Table I) and CarB (Table I, see also Fig. 1 *g*). The mouse 10T1/2 fibroblasts were used as a negative control. The levels of E-cadherin protein detected in whole cell extracts from PDV and PDVC57 cells were surprisingly low, as compared with the immunofluorescent analysis (see Fig. 1), which could suggest a stronger association of E-cadherin to cytoskeletal components in those cell lines. However, solubilization experiments of the E-cadherin protein with the detergent NP-40 (Hirano et al., 1987; Nagafuchi and Takeichi, 1988) showed that the low amounts of E-cadherin detected in whole cell extracts of PDV and PDVC57 cells cannot be explained by such an association. In fact, lower levels of insoluble E-cadherin and a higher proteolytic sensitivity of the soluble component were detected in PDV and PDVC57, as compared with MCA3D and AT5 cells (not shown).

In contrast to the above results, no correlation between the amount of solubilized P-cadherin protein and tumorigenicity was found in the cell lines which exhibited an epithelial or epithelioid morphology (Fig. 3 *C*, Table I); high levels of the protein were detected in MCA3D, AT5, PDV, and HaCa4 cells, and lower in PDVC57 cells. However, no P-cadherin was detected in CarC (Fig. 3 *C*, Table I) and CarB cell (Table I), in agreement with the immunofluorescent analysis.

Northern and Southern Studies

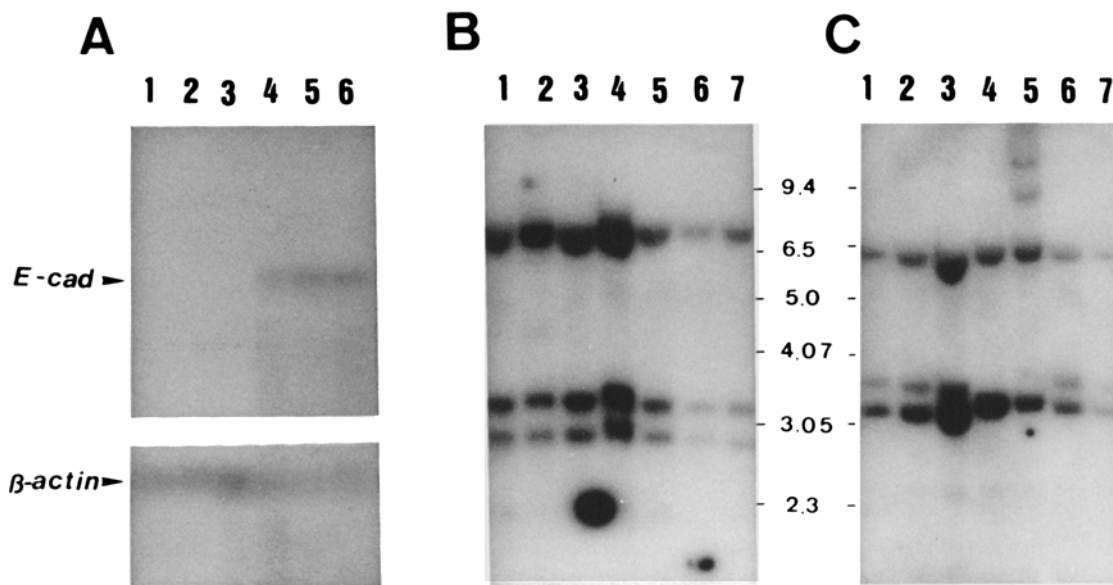The amount of E-cadherin mRNA in the various cell lines

Figure 4. Northern and Southern blot analysis of the keratinocyte cell lines for E-cadherin mRNA expression and genomic organization. (*A*) Northern blot containing total cellular RNA (10 μg per lane) from the different cell lines were hybridized with the E-cadherin cDNA probe (0.9-kb BamHI fragment from pBATEM2 vector) and with a rat β-actin cDNA probe (0.6-kb EcoRI-HindIII fragment). Migration of the E-cadherin mRNA (4.5 kb) and β-actin mRNA (2.0 kb) are indicated by arrowheads on the left. (*B* and *C*) Genomic DNA isolated from the different cell lines was digested with an excess of BamHI (*B*) or EcoRI (*C*) restriction enzymes and hybridized to the E-cadherin cDNA probe. Migration of pBR322-EcoRI and λ-HindIII markers are indicated between *B* and *C*. RNAs (*A*) and/or DNAs (*B* and *C*) were extracted from: lane *1*, CarB; lane *2*, CarC; lane *3*, HaCa4; lane *4*, PDVC57; lane *5*, PDV; lane *6*, AT5; and lane *7*, MCA3D cells. The two large fragments, detected exclusively in EcoRI-DNA from PDV cells (C.5), arise from incomplete DNA digestion of this particular sample. The E-cadherin mRNA is not expressed in the three carcinoma cell lines. Apparently no deletions or rearrangements detected by BamHI or EcoRI enzymes are observed in the carcinoma cell lines.

was analyzed by Northern blot hybridization using a specific cDNA probe (see Materials and Methods). A band of 4.5-kb was detected in AT5, PDV, and PDVC57 cells (Fig. 4 *A*, lanes *6*, *5*, and *4*, respectively, see also Fig. 7, lane *1*, for MCA3D cells), with similar relative abundance in AT5 and PDV cells and slightly lower levels in PDVC57 cells. The size of this mRNA is identical to that previously reported for mouse E-cadherin mRNA (Nagafuchi et al., 1987). None of the carcinoma-derived cells, CarB, CarC, and HaCa4, contained detectable levels of this mRNA (Fig. 4 *A*, lanes *1–3*), whereas they expressed high levels of the 2.0-kb β-actin messenger, used as an internal control (Fig. 4 *B*). This suggested that, in carcinoma-derived cells, the absence of E-cadherin protein synthesis might occur at the mRNA transcriptional level (or mRNA stability) and prompted us to study the genomic integrity of the E-cadherin gene.

It has been clearly established that chromosomal aberrations, involving gross alterations of DNA sequences such as deletion, amplification, or translocation, are frequently observed in mouse skin carcinogenesis (Conti et al., 1986; Aldaz et al., 1989). Genetic changes affecting specific genes, such as the H-ras oncogene, have also been reported in this system (Quintanilla et al., 1986; Bremner and Balmain, 1990). To analyze the integrity of the E-cadherin gene in the carcinoma cell lines, we compared the restriction patterns of DNA isolated from the cells after digestion with BamHI or EcoRI enzymes by Southern blots. As shown in Fig. 4 *B*, the same BamHI restriction pattern with fragments of approximately 6.7, 3.2, and 2.8 kb, was observed in all cell lines. A similar result was obtained with EcoRI-digested DNA (Fig.

4 *C*), where only minor differences in the number and the mobilities of the DNA fragments were observed in the PDV and PDVC57 cell lines (a single fragment of ~3.4 kb instead of the two 3.6- and 3.3-kb fragments detected in the other cell lines; Fig. 4 *C*, lanes *4* and *5*). These differences can be explained by the EcoRI polymorphism for the E-cadherin gene previously identified in the C57BL/6 mouse strain (Eistetter et al., 1988), from which both PDV and PDVC57 cell lines were derived (Fusenig et al., 1982; Bremner and Balmain, 1990; Quintanilla et al., 1991).

These results clearly suggest that the absence of E-cadherin expression observed in carcinoma-derived cells cannot be explained on the basis of large rearrangements or deletions affecting the E-cadherin gene, but rather point to inactivation of gene expression. The latter situation appears to be true, at least for HaCa4 cells, since reexpression of the E-cadherin gene takes place in tumors induced by this cell line (see below).

Expression of E- and P-Cadherin in Nude Mouse-induced Tumors

When the tumors induced by the cell lines in nude mice were immunohistochemically stained with the mAb ECCD-2, we observed that certain regions of the tumors induced by HaCa4 cells were positive for E-cadherin, indicating that expression of E-cadherin was reactivated in an in vivo environment. The staining, however, was restricted to the central differentiated regions and was completely absent from the highly anaplastic periphery of the tumors (Fig. 5 *e*).

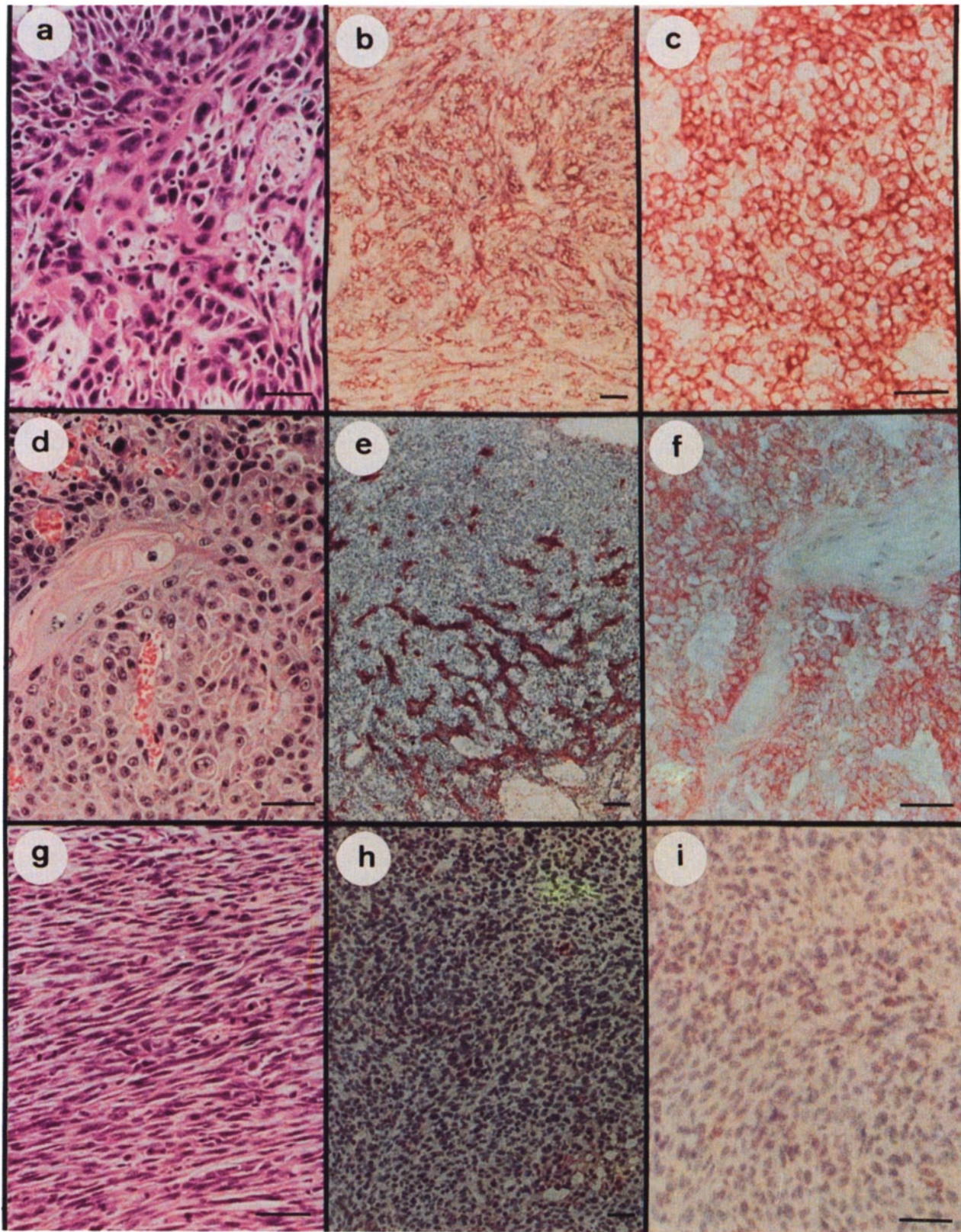The E-cadherin immunostaining pattern of HaCa4 in-

Figure 5. Histology and immunohistological localization of E- and P-cadherin in nude mouse-induced tumors by the epidermal cell lines. (*a–c*) PDV-induced tumors; (*d–f*) HaCa4-induced tumors; (*g–i*) CarB-induced tumors. (*a, d,* and *g*) Histological analysis of paraffin-embedded material. (*b, e,* and *h*) E-cadherin immunostaining. (*c, f,* and *i*) P-cadherin immunostaining. E- and P-cadherin were stained on frozen material with the mAb ECCD-2 and PCD-1, respectively, using a biotin-extravidin-alkaline phosphatase complex. Induction of E-cadherin expression takes place in reduced areas of tumors induced by HaCa4 cells. Complete absence of E- and P-cadherin was detected in spindle cell carcinomas induced by CarB cells. Bar, 150 μm.

duced tumors was different from that of PDV (Fig. 5 *b*) and PDVC57 (not shown) tumors, where E-cadherin appeared more widely and homogeneously distributed. A semiquantitative estimation of E-cadherin staining in the tumor sections suggests a range of protein expression similar to that observed in the cultured cell lines with PDV greater than that of PDVC57 which is much higher than that of HaCa4. In all of these tumors, classified as squamous cell carcinomas by histological criteria (see Fig. 5, *a* and *d*), E-cadherin immunostaining was always detected at the cell–cell contact areas of differentiating and keratinizing regions and was absent from the more anaplastic cells (see Fig. 5 *e*, see also Fig. 8 *b*).

On the contrary, immunohistochemical staining of PDV and HaCa4-tumors with the mAb PCD-1, showed that P-cadherin protein was homogeneously distributed throughout the tumor sections and absent from the keratinized areas (Fig. 5, *c* and *f*). Identical results were obtained with PDVC57 tumors (not shown). No differences in PCD-1 staining were observed in tumors induced by PDV, PDVC57, and HaCa4 cells.

Complete absence of E- and P-cadherin protein expression was observed in tumors induced by the fibroblast-like CarB and CarC cells, as exemplified for one CarB-induced tumor shown in Fig. 5, *h* and *i*. Tumors induced by these two cell lines were classified as spindle cell carcinomas (Fig. 5 *g*), in agreement with the origin of both cell lines (Quintanilla et al., 1986).

Introduction of Exogenous E-Cadherin cDNA into HaCa4 Cells Confers a More Epithelial Phenotype and Partially Suppresses Tumorigenicity

To examine whether or not the forced expression of E-cadherin could change the tumorigenic potential of carcinoma cells, we chose the E-cadherin-negative, P-cadherin-positive, highly malignant HaCa4 cell line.

HaCa4 cells were cotransfected with the pBATEM-2 and pSV2neo vectors that contain the complete E-cadherin cDNA sequence (Nose et al., 1988) and a neomycin-resistance gene (Southern and Berg, 1982), respectively. Neomycin-resistant colonies were isolated and selection of the E-cadherin-expressing clones was carried out by immunofluorescence and Western immunoblotting. Some clones showed a marked morphological change to a more epithelial phenotype compared to the parental HaCa4 cells. The selected transfectants were further subcloned by limiting dilution.

Characterization of the Transfectants

Clones neo3 and neo2 were selected after transfection of HaCa4 cells with the neomycin-resistance vector alone and were used as controls in all subsequent analyses. Clone E5 was isolated because, although presenting a HaCa4-like phenotype and negative immunofluorescent staining with the mAb ECCD-2, it contained detectable amounts of soluble E-cadherin by Western blot analysis (not shown). Subclones E54 and E58 were further isolated from the E5 clone, and characterized as E-cadherin positive (E-cad+) and E-cadherin negative (E-cadh−), respectively. Subclones E62 and E24, both E-cad+, were isolated from independent clones. Fig. 6 shows the morphology and the patterns of E- and P-cadherin immunofluorescence of various transfectants. As

can be observed, the E-cad+ transfectants E62 (Fig. 6 *d*) and E24 (Fig. 6 *g*) presented an apparent change in their morphological phenotype compared with the control neo3 (Fig. 6 *a*) or the parental HaCa4 cells (see Fig. 1 *f*). Clear and defined islands with strong intercellular contacts could easily be observed when the E-cad+ subclones were grown at low density, in contrast with the behavior of HaCa4 cells. A similar morphological change was also observed in the E-cad+ E54 transfectant subclone (not shown). In contrast, the E-cad− subclone E58 showed the same morphological phenotype as control cells (Fig. 6 *j*). Immunofluorescence analyses of the various cell clones using the mAb ECCD-2 showed that E62, E24 (Fig. 6, *e* and *h*) and E54 (not shown) exhibited positive staining for E-cadherin at the cell–cell contact areas, whereas clones neo3 and E58 (Fig. 6, *b* and *k*) remained negative as the parental HaCa4 cell line (see Fig. 1 *e*). On the other hand, staining with the mAb PCD-1 showed that all transfectants remained positive for P-cadherin (Fig. 6, *c*, *f*, *i*, and *l*), as expected.

Expression of E-cadherin in the transfectants was further analyzed by Northern blot hybridization. As shown in Fig. 7 *A*, one specific band could be detected in the lanes corresponding to the E-cad+ transfectant clones, although at variable intensities. The size of the E-cadherin mRNA detected in the clones E5, E62, and E54 was ∼3.9 kb (Fig. 7 *A*, lanes *3*, *4*, and *5*, respectively), smaller than the endogenous E-cadherin mRNA (4.5 kb), of MCA3D cells (Fig. 7 *A*, lane *1*, see also Fig. 4 *A* for the other cell lines). Surprisingly, the size of the E-cadherin mRNA detected in clone E24 (4.5 kb) (Fig. 7 *A*, lane *2*) corresponded to that of the endogenous mRNA, suggesting that this particular subclone had somehow switched on the endogenous E-cadherin gene during the transfection experiment. However, Western blot analysis for E-cadherin protein revealed that all E-cad+ transfectants synthesized a 124-kD reactive polypeptide, regardless of the size of their E-cadherin mRNA (Fig. 7 B, lanes *3–5*).

To characterize the genomic integration of the exogenous cDNA, Southern blot analyses were carried out. As can be observed in Fig. 7 *C*, the BamHI patterns of DNA digested from clones E62, E54, and E5 contained an additional hybridizing fragment of ∼0.9 kb, besides the normal 6.7-, 3.2-, and 2.8-kb fragments (see also Fig. 4 *C*, for parental HaCa4 DNA). The intensity of the 0.9-kb fragment was very weak, although detectable, in DNA from clone E5 (Fig. 7 *C*, lane *3*) and strong in DNA from clones E62 and E54 (Fig. 7 *C*, lanes *4* and *5*, respectively). The 0.9-kb band corresponds exactly to the expected size of the major fragment generated from the exogenous E-cadherin cDNA after BamHI digestion (Nagafuchi et al., 1987). Thus, the presence of this fragment is considered as diagnostic of the integration of the pBATEM-2 vector. This diagnostic 0.9-kb band was detected neither in DNA from the clones E24, E58, neo3 (Fig. 7 *C*, lanes *2*, *6*, and *7*, respectively), nor in that of the parental HaCa4 cells (see Fig. 4 *C*, lane *3*). An additional fragment of ∼2.7 kb was also detected in the BamHI pattern of DNA from E62 and E54 subclones (Fig. 7 *C*, lanes *4* and *5*), although at lower intensity than the 0.9-kb band. This 2.7-kb fragment probably arose from partial digestion of the cDNA. Similar results were obtained from Southern blots after EcoRI digestion; a diagnostic band of 2.6 kb was detected in DNA samples from clones E62, E54, and E5, but was completely absent in DNA from clones E58, E24, and neo3 (not shown).
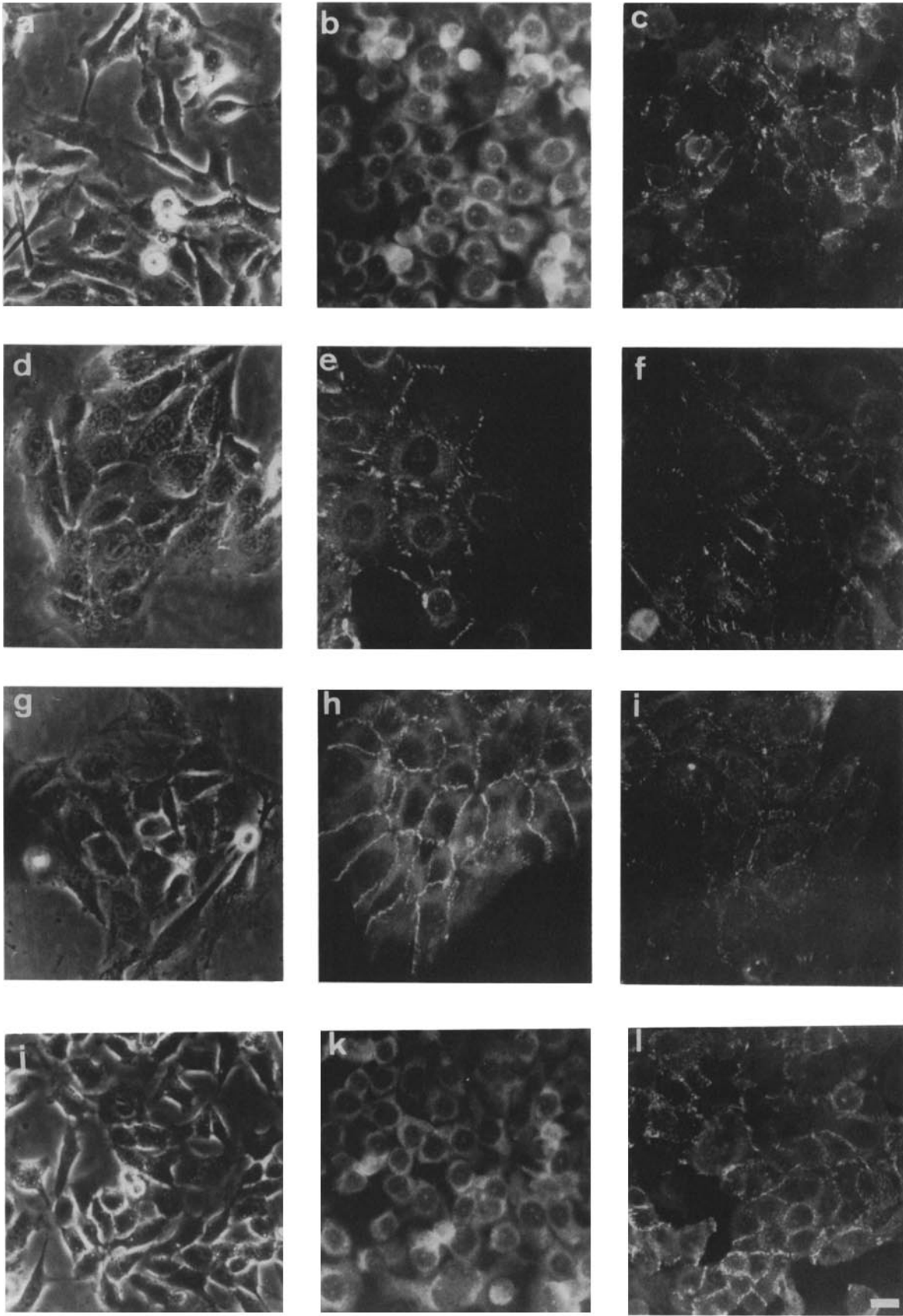
Figure 6. Morphological phenotype and immunofluorescent staining for E- and P-cadherin in HaCa4-transfectant cell clones. (*a–c*) Control clone HaCaneo3; (*d–f*) transfectant clone E62; (*g–i*) transfectant clone E24; (*j–l*) transfectant clone E58. (*a, d, g,* and *j*) Phase-contrast images of living cells. (*b, e, h,* and *k*) Immunofluorescent staining with the mAb ECCD-2. (*c, f, i,* and *l*) Immunofluorescent staining with the mAb PCD-1. E-cadherin is expressed at the areas of cell–cell contacts in the E62 and E24 transfectants. Bar, 45 μm.
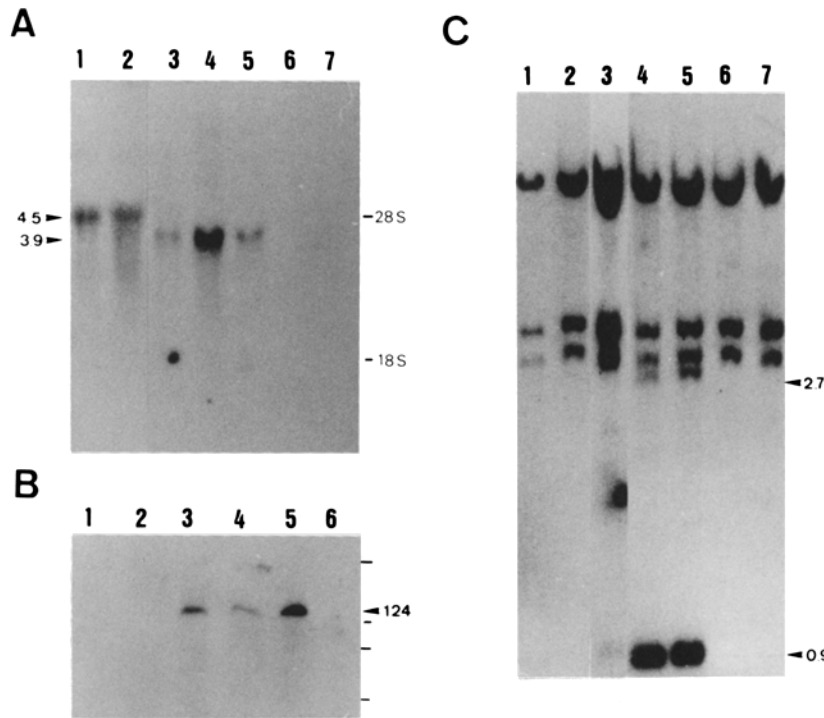
A

B

C

Figure 7. Northern, Western, and Southern blot analyses of the HaCa4-transfectant cell clones for E-cadherin. (*A*) Northern blot of total cellular RNA (10 μg per lane) from the different transfectant cell clones with the E-cadherin cDNA probe. (*B*) Western immunoblotting analysis with the mAb ECCD-2. (*C*) BamHI restriction pattern of DNA samples from the transfectants for E-cadherin. RNA (*A*) and DNA (*C*) were isolated from: lane *1*, control cell line MCA3D; lane *2*, transfectant clone E24; lane *3*, transfectant clone E5; lane *4*, transfectant clone E62; lane *5*, transfectant clone E54; lane *6*, transfectant clone E58; and lane *7*, control clone neo3. (*B*) Whole cell extracts obtained in the presence of 10 mM CaCl$_2$ and protease inhibitors from: lane *1*, parental HaCa4 cells; lane *2*, control clone neo3; lane *3*, transfectant clone E54; lane *4*, transfectant clone E24; lane *5*, transfectant clone E62; and lane *6*, transfectant clone E58. Migration of E-cadherin polypeptide (124 kD) is indicated by an arrowhead and that of molecular mass markers, 205, 116, 97.4, and 66 kD by small marks on the right. The transfectant clone E24 has not integrated the exogenous E-cadherin cDNA, but activated the endogenous E-cadherin gene. All E-cad+ transfectants express the same 124-kD immunoreactive polypeptide.

These results unambiguously demonstrate that subclones E62, E5, and E54 have stably integrated the exogenous E-cadherin gene, although at variable copy numbers. In contrast, the subclone E24 did not take up the exogenous cDNA, but activated the endogenous E-cadherin gene, expressing high levels of E-cadherin mRNA and protein. The subclone E58 neither integrated the exogenous cDNA nor switched on the endogenous E-cadherin gene, and its behavior is similar to that of the neo3 clone transfected with the neomycin vector alone.

Tumorigenicity of the Transfectants and Expression of E-cadherin in Nude Mouse-induced Tumors

The tumorigenic capability of the various transfectant cell lines was tested in nude mice using a double strategy. One series of mice was double injected as follows: each mouse received 1 × 10⁶ cells of the control clone neo3 (or neo2) in the left flank and the same number of cells of each of the E-cad+ or E-cad− transfectants in the right flank. The animals were killed when tumors in any flank reached a size

Table II. Size of Tumors in Double-injected Nude Mice*

Mouse number	Cell line	Tumor size	Cell line	Tumor size	Volume‡ ratio
		cm		*cm*	
Experiment I					
1	neo3	1.5 × 1.0 × 1.0	HaCa4	2.0 × 1.0 × 1.0	0.75
2	neo2	1.5 × 1.0 × 0.8	HaCa4	2.0 × 1.2 × 1.0	0.5
3	neo3	2.0 × 1.0 × 1.0	E5	2.3 × 1.0 × 0.8	0.92
4	neo3	2.0 × 1.3 × 1.0	E62	0.5 × 0.4 × 0.3	43
5	neo3	2.0 × 1.5 × 1.0	E24	No tumor	
Experiment II					
1	neo3	1.3 × 1.0 × 1.0	E58	1.5 × 1.3 × 1.2	0.55
2	neo3	2.2 × 1.5 × 1.4	E58	2.0 × 1.3 × 1.1	1.6§
3	neo3	1.5 × 1.5 × 0.6	E54	0.6 × 0.4 × 0.3	19
4	neo3	2.0 × 1.7 × 1.0	E54	1.1 × 0.6 × 0.5	10.3‖

* Each mouse was injected with 1 × 10⁶ cells of clone neo3 (or neo2) in the left flank and with the same number of cells of the other cell lines in the right flank. Animals were sacrificed 9–11-d postinjection, except when indicated, and the excised tumors measured in three dimensions. Data of tumor sizes for each individual mouse are presented in the same row.
‡ The volume of each tumor was estimated from measures in three dimensions. The volume ratio was established as the ratio between the volume of the tumor developed on the left flank and the volume of the tumor developed on the right flank.
§ The mouse was sacrificed at day 21 after injection. The estimated latency of tumors were 10 d for neo3 and 12 d for E58.
‖ The mouse was sacrificed at day 16 after injection. The estimated latency of tumors were 10 d for neo3 and 15 d for E54.

Table III. Latency and Growth of Tumors in Single-injected Nude Mice

Mouse number	Cell line	Size of tumors after injection day (in centimeters)*							
		7 d	8 d	9 d	11 d	15 d	19 d	21 d	23 d
Expt. I									
1	HaCa4	0.5	0.7	1.0	1.7‡				
		0.5	0.8	1.0	2.0				
		0.2	0.5	0.8	1.5				
2	E5	0.5	1.0	2.5‡					
		0.2	0.4	0.7					
		0.2	0.8	1.2					
3	E62	0.3	0.5	0.7	1.0	1.7‡			
		−	0.2	0.3	0.3	1.0			
		−	−	0.2	0.3	1.0			
4	E24	−	−	−	−	0.1	0.7	1.0	1.5‡
		−	−	−	−	0.1	0.7	1.0	1.3
		−	−	−	0.1	0.2	0.8	1.2	1.5
Expt. II									
1	E58	0.3	0.5	0.9	1.2‡				
		0.3	0.4	0.7	1.0				
		0.5	0.7	1.0	1.7				
2	E54	−	−	0.1	0.2	0.6	1.0	1.3‡	
		0.1	0.2	0.4	0.6	0.8	1.2	1.5	
		−	−	0.2	0.3	0.7	1.1	1.5	
3	E24$_{nm}$	−	−	−	−	−	1.5	2.0‡	
		−	−	0.1	0.2	1.0	1.3	1.6	
		0.2	0.4	0.4	0.5	1.0	1.5	1.7	
Expt. III									
1	HaCa4	0.4	0.7	1.0	1.5‡				
		0.4	0.8	1.0	1.5				
		0.5	1.0	1.2	1.7				
2	E62	0.3	0.5	0.7	1.0	2.3‡			
		−	−	0.2	0.4	2.0			
		−	−	−	0.1	1.0			
3	E62$_{nm}$	0.4	0.6	1.0	2.0	2.5‡			
		0.2	0.2	0.4	0.5	1.2			
		−	−	−	−	0.2			

* Each mouse was injected subcutaneously with the various cell lines at three sites, the two flanks and the neck (1 × 10⁶ cells per injection site). Animals were examined daily and the size of tumors was estimated as the higher outer diameter. The estimated size of tumors in the three sites of each individual mouse at different days after injection is presented.
‡ Symbols indicate the date on which the mice were killed.

between 1.5 and 2 cm. The results from two experiments are summarized in Table II. From a total of 10 animals, 8 were killed at 9–11-d postinjection, and the other 2 animals survived for a longer period of 16 and 21 d. The tumorigenicity of the control clone neo3 (and neo2) was very close to that of the parental HaCa4 cells, giving rise to tumors of ∼1 cm in size within the first 7–9 d. The transfectant cell clones which were E-cad− (such as E58), or weakly positive (such as E5) gave rise to tumors with similar latency periods and growth rates as neo3 or the parental HaCa4 cells. In contrast, all of the E-cad+ clones (E62, E54, and E24) gave rise to tumors with longer latency periods and a slower growth rate. As can be seen in Table II, all tumors induced by the control cells neo3 reached a size at least 10 times larger than those induced by E-cad+ cells at the killing date.

A second series of mice was individually injected with each of the different cell clones at three sites. The animals were examined daily and sacrified when at least two of the sites developed tumors of ∼1.5–2 cm. Examples of three separate experiments are presented in Table III. Parental HaCa4 cells and E-cad− clones induced tumors with very

short latency periods and a fast growth rate (the doubling rate was ∼2 d) and all animals had to be killed within 9–11-d postinjection. Animals injected with E-cad+ clones survived for at least 15 d and, in general, the tumors developed with longer latency periods and slower growth rates as compared with those induced by E-cad− cells. The data in Table III (experiments II and III) include two new cell lines (E24nm and E62nm), derived from nude mouse tumors induced by clones E24 and E62, respectively. As can be observed, both cell lines showed a tumorigenic behavior similar to that of the parental clones.

A summary of the results of these assays, which includes the total number of tumors induced by the different clones, is presented in Table IV. A clear-cut difference can be established between the tumorigenicity of E-cad− and E-cad+ cells. At least 60% of the tumors induced by E-cad− cells reached a size of 1 cm between 7 and 9 d after injection. The remainder of the tumors reached that size at day 11. In contrast, all tumors induced by E-cad+ cells developed with latency periods longer than 10 d, with a variable distribution between the different transfectants. E62-tumors have shorter

Table IV. Summary of the Latency of the Total Tumors Analyzed*

Cell line	E-cadherin‡ expression	Latency to reach 1 cm in size				Total number tumors (injection sites)	Number of mice
		7–9 d	10–14 d	15–20 d	>20 d		
HaCa4	−	7	1			8(8)	4
neo3	−	5	3			8(8)	8
E5	±	3	1			4(4)	2
E58	−	3	2			5(5)	3
E54	+ + +			4	1	5(5)	3
E62	+ + +		6§	4		10(10)	4
E62nm	+ + +		5	1‖		6(6)	2
E24	+ +				3	3(4)¶	2
E24nm	+ +			5	1	6(6)	2

* The total number of tumors induced by the transfectants which reached 1 cm in size (latency) at the indicated days after injection is presented. The figures include those presented in Tables II and III, and additional data on single-injected animals.

‡ The + and − symbols represent the relative levels of E-cadherin protein expressed by the different cell lines in culture, derived from immunofluorescence and Western blotting data.

§ The tumor induced by E62 in a double-injected mouse (neo3/E62) reached a size of 0.5 cm when the mouse was sacrificed 9 d after injection (see Table II, experiment I, Mouse 4).

‖ The tumor had reached a size of ∼ 0.2 cm when the mouse was killed 15 d after the injection (see Table III, Experiment III, Mouse 3).

¶ The mouse double-injected with neo3/E24 did not develop a tumor on the right flank when it was killed 9 d after the injection (see Table II, Experiment I, mouse 5).

latency periods (10–14 d in 60% of the cases) than those induced by E54 cells (15–20 d in 80% of the tumors). The most striking differences were found with the E24 clone, which induced tumors with latency periods longer than 20 d and slow growth rates (see Table III, Expt. 1, mouse 4).

From these experiments, we can conclude that the forced expression of E-cadherin leads to a partial suppression of the tumorigenicity of the highly malignant HaCa4 carcinoma cell line.

Histological analysis of the tumors induced by the different transfectant cell clones indicated that all were squamous cell carcinomas (Fig. 8, a, d, and g), as the parental HaCa4 cell line (see Fig. 5 d). Immunohistochemical analysis of the tumors with the mAb ECCD-2 showed that all tumors expressed E-cadherin at variable levels. Tumors induced by the control clone neo3 showed a pattern of E-cadherin staining (Fig. 8 b) very similar to that of HaCa4-induced tumors; a small number of E-cadherin expressing cells restricted to the more differentiated and keratinized regions of the tumors. The same result was obtained in tumors induced by the E-cad− clone E58 (not shown). Tumors induced by E-cad+ clones, such as E62, showed stronger staining for E-cadherin and a more homogeneous distribution throughout the tumor sections. Most of the cells of E62 tumors, including the less-differentiated ones, exhibited positive staining at the cell–cell contact areas, and the intensity of staining increased in the more differentiated and keratinized regions of the tumor (Fig. 8 e). High levels of E-cadherin expression were also detected in E24-induced (Fig. 8 h) and E54-induced (not shown) tumors, although in these two cases the staining appears exclusively localized to the differentiating regions.

Immunohistochemical staining of the tumors with the mAb PCD-1 showed that both the intensity and the pattern of P-cadherin staining was very similar in all tumors induced by either E-cad+ or E-cad− transfectant cells. High and homogeneous expression of P-cadherin was detected in all regions of the tumors, except in keratinazed areas from which it was excluded (Fig. 8, c, f, and i). This is the same pattern detected in tumors induced by the parental HaCa4 cells (see Fig. 5 f).

Discussion

Mouse epidermal carcinogenesis is an invaluable model system for the study of molecular events associated with tumor progression. In the present report, we have addressed the role of calcium dependent cell–cell adhesion molecules in carcinogenesis by analyzing the expression of E- and P-cadherins in a series of mouse epidermal cell lines representative of different stages of tumor progression and in tumors induced by injection of cells in nude mice. We have found an inverse correlation between the levels of solubilized E-cadherin and the tumorigenicity of the cell lines (Table I). In addition, a complete absence of E-cadherin protein and mRNA was observed in the three carcinoma cell lines analyzed (HaCa4, CarB, and CarC) (see Figs. 1, 3 B, and 4 A). In contrast, no apparent correlation was detected between P-cadherin protein levels and tumorigenicity. The highly tumorigenic HaCa4 cells expressed P-cadherin at even higher levels than the nontumorigenic MCA3D. However, P-cadherin was absent in two carcinoma cell lines, CarB and CarC (Figs. 2 and 3 C).

HaCa4 cells derive from a squamous cell carcinoma induced by treatment of mouse skin with the HaMSV retrovirus and TPA (Brown et al., 1986); they present an epithelioid morphology in culture (Fig. 1 f) and are highly tumorigenic in nude mice. The CarB and CarC cell lines originated from two independent, highly malignant spindle cell carcinomas induced by DMBA/TPA treatment (Quintanilla et al., 1986) and, consequently, exhibit a fibroblastoid phenotype in culture (see Fig. 1 h and Fig. 2, f and i). The correlation observed between decreased amounts of E-cadherin protein and the tumorigenicity of the cells, together with the finding that E-cadherin expression is absent from cultured carcinoma cells, suggest a role for this cell–cell adhesion molecule in the progression to malignancy of mouse epidermal carcinogenesis.
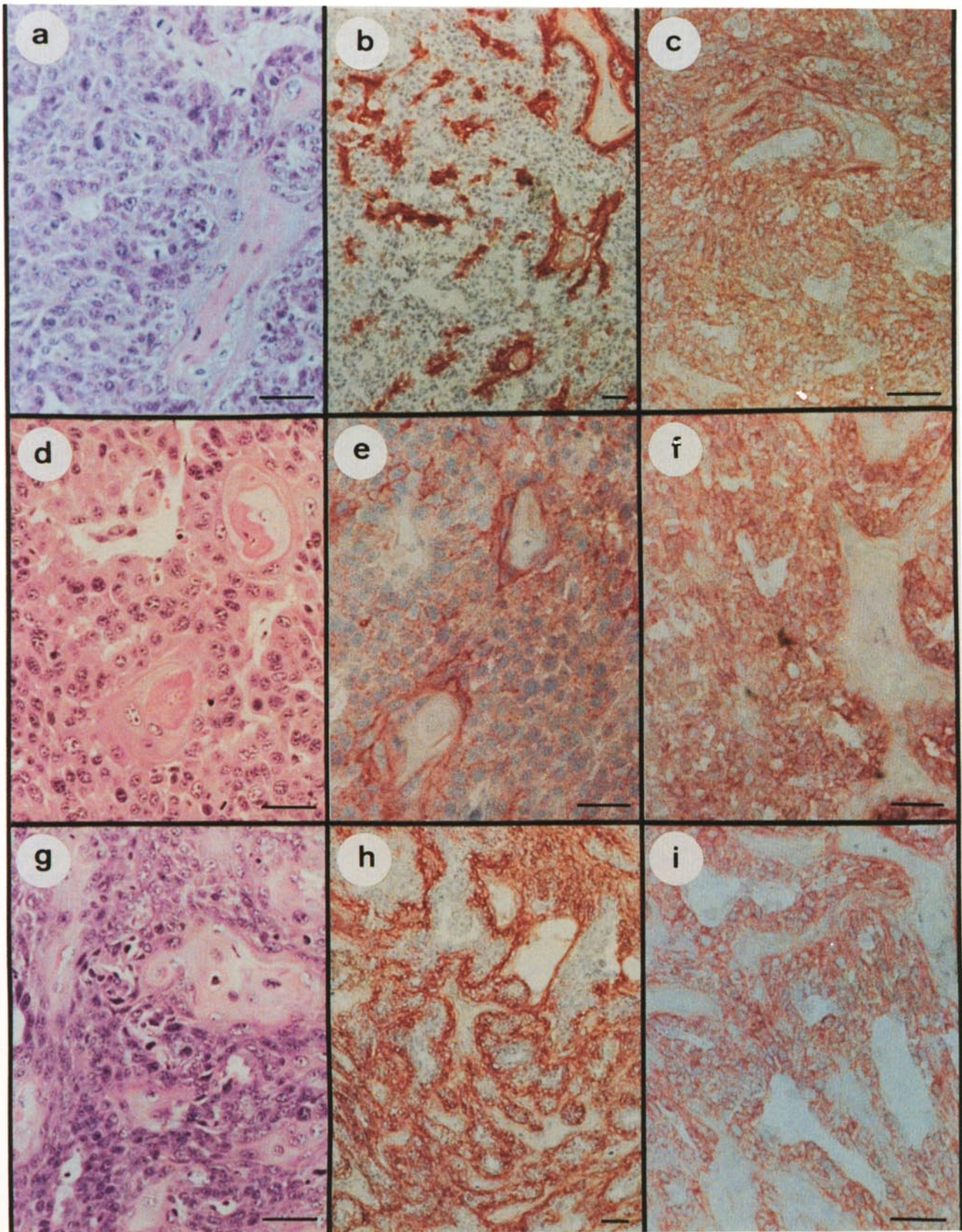
Figure 8. Histology and immunohistochemical localization of E- and P-cadherin in nude mouse-induced tumors by HaCa4-transfectant cell clones. (*a–c*) Tumors induced by control clone neo3; (*d–f*) tumors induced by clone E62; (*g–i*) tumors induced by clone E24. Immunostaining for E- and P-cadherin was carried out as in Fig. 5. (*a, d,* and *g*) Histological analysis of paraffin-embedded material. (*b, e,* and *h*) E-cadherin staining. (*c, f,* and *i*), P-cadherin staining. Bar, 150 μm.

Another interesting point that emerges from this study is a possible role for E- and P-cadherin in the maintenance of cell shape. All the epidermal cells which express both E- and P-cadherin (MCA3D, AT5, PDV, and PDVC57) exhibit a typical epithelial morphology with a cobblestone pattern of growth, and express high amounts of cytokeratin (Díaz-Guerra, M., C. Bauluz, S. Haddow, J. L. Jorcano, A. Cano, A. Balmain, and M. Quintanilla, manuscript submitted for publication). Switching off the expression of both cadherins correlates with a fibroblastoid morphology and with a highly malignant behavior, exemplified by the CarB and CarC cell lines. The HaCa4 cells represent an intermediate stage, with tumorigenic properties of carcinoma cells related to the absence of E-cadherin, but exhibiting an epithelioid morphology which can be explained by the high amounts of P-cadherin expressed.

These results are, in principle, in agreement with recent reports which suggest an anti-invasive role for E-cadherin (Behrens et al., 1989; Frixen et al., 1991). However, in those studies with H-ras-transformed MDCK cells (Behrens et al., 1989) and with human carcinoma cell lines (Frixen et al., 1991), a direct correlation between the loss of E-cadherin expression and acquisition of an invasive fibroblastoid phenotype has been reported. We show here that this is not always the case and that, at least in epidermal cells, the phenotypic epithelioid-fibroblastoid conversion appears to be related with the loss of both E- and P-cadherin.

The analyses of E-cadherin gene organization in the epidermal cell lines by Southern blot hybridization suggest that E-cadherin gene inactivation in mouse carcinoma cells (see Fig. 4, B and C) can be explained at the transcriptional level (or mRNA stability) as reported by Frixen et al. (1991) in human carcinoma cells. We have also found support for this hypothesis from our studies on E-cadherin expression in nude mouse tumors induced by these cell lines. Immunohistochemical staining of tumor sections with the mAb ECCD-2 showed that reexpression of E-cadherin takes place in reduced areas of the tumors induced by HaCa4 cells. These observations support the existence of a transcriptional block in cultured HaCa4 cells and that the E-cadherin gene can be activated in an in vivo environment.

However, when the relative levels of E-cadherin protein were compared in stained sections of different tumors, we observed the same inverse correlation as in cultured cells. Thus, the overall levels of E-cadherin protein were relatively high and homogeneous in well-differentiated squamous cell carcinomas induced by PDV and PDVC57 cells and decreased in the moderately differentiated squamous cell carcinomas induced by HaCa4 cells (compare in Fig. 5, b and e). In all the squamous cell carcinomas analyzed, E-cadherin staining was located at the cell-cell contact regions of differentiating cells, reproducing the expression pattern observed in normal epidermis (Nose and Takeichi, 1986). In addition, poorly differentiated spindle cell carcinomas induced by the CarB and CarC cell lines were completely negative for both E- and P-cadherin staining (Fig. 5, h and i). These observations suggest that instability, or even the complete switching off, of E-cadherin expression can be associated with progression to malignancy. In agreement with our results, low and unstable expression of E-cadherin has also recently been reported to occur in highly metastatic derivatives of a murine ovarian carcinoma cell line (Hashimoto

et al., 1989). However, it is presently unknown if such instability is the consequence of alterations of specific transcriptional factors or due to posttranscriptional mechanisms leading to downregulation of the protein.

We have examined the influence of E-cadherin on the tumorigenic potential of carcinoma cells by introducing an exogenous E-cadherin cDNA into the HaCa4 cell line. E-cad+ HaCa4 transfectants showed a partial suppression of the tumorigenicity, giving rise to tumors with longer latency periods and a higher differentiation grade compared with the parental HaCa4 cells or control cells transfected with a neomycin resistance vector alone. Interestingly, the most noticeable effect in the suppression of tumorigenicity was observed in the transfectant E24, which has not incorporated the exogenous E-cadherin cDNA, but, for unknown reasons, has switched on its endogenous E-cadherin gene (see Fig. 7, A and C, lanes 2). One possible explanation for this behavior could reside in a higher stability and/or stronger association to the cytoskeleton of the endogenous versus the exogenous protein. We are presently investigating this point in greater detail.

The mouse skin carcinogenesis model is being exhaustively studied in several laboratories to elucidate the molecular events associated with tumor development and progression. Activation of the H-ras protooncogene is a frequent event at the initiation stage induced by DMBA (Quintanilla et al., 1986; Brown et al., 1990), but this activation is not sufficient to confer a full neoplastic phenotype on the initiated cells (Quintanilla et al., 1991). Although further changes in the H-ras gene locus can influence tumor progression (Bremner and Balmain, 1990), other genetic events other than ras remain to be discovered. Thus, the inactivation of tumor suppressor genes has been proposed to occur during progression from papillomas to carcinomas (Bremner and Balmain, 1990; Bianchi et al., 1990). All cell lines used in the present study, except the nontumorigenic MCA3D cells, bore different alterations in the H-ras gene (Quintanilla et al., 1986, 1991; Bremner and Balmain, 1990). In contrast to the results reported for MDCK cells (Behrens et al., 1989), we show here that transfection of a H-ras oncogene into MCD3D cells does not confer a fibroblastoid phenotype nor inactivates E-cadherin expression. In fact, the transfectants, as exemplified here by AT5 cells, remain epithelial, contain high amounts of E-cadherin, and are weakly tumorigenic in nude mice. Another example is provided by the cell line PDV and its derivative PDVC57 in which an increase in the H-ras mutant gene and p21 mutated product occur in PDVC57 cells (Bremner and Balmain, 1990; Quintanilla et al., 1991). However, both cell lines remain epithelial and contain detectable amounts of E-cadherin protein. These observations imply that activation of the H-ras protooncogene in this system is not sufficient for switching off E-cadherin expression. Although a possible influence of H-ras alterations on the stability of the protein cannot be presently discarded, further molecular events associated with progression of malignancy could account for the deregulation of E-cadherin expression in carcinoma cells.

Recent studies in mouse skin carcinogenesis indicate that loss of heterozygosity of chromosome 7, where the H-ras gene is located, is a frequent event in the final stages of tumor progression (Aldaz et al., 1989; Bremner and Balmain, 1990; Bianchi et al., 1990). These observations support the

existence of a putative tumor suppressor gene on chromosome 7, linked to the H-ras gene locus, involved in mouse epidermal carcinogenesis. The relevance of this suggestion relies in the fact that chromosome 7 is the murine homologue to human chromosome 11 where at least two putative tumor suppressor genes are located (Koufos et al., 1989; Haber et al., 1990). The results reported here suggest that the putative murine tumor suppressor gene could be involved in the regulation of the differentiation state of the epidermal cells. Such a differentiation gene may regulate, directly or indirectly, the expression of E- and P-cadherins, as well as other epithelial markers such as the cytokeratins. In this sense, the progression from squamous cell carcinomas to spindle cell carcinomas, considered the final stage of tumor progression in mouse epidermal carcinogenesis, involves the progressive loss of cytokeratins (Klein-Szanto et al., 1989) together with the suppression of E- and P-cadherin expression (this paper). For instance, the CarB and CarC cell lines still express minor amounts of cytokeratins, including the simple epithelial cytokeratin CK8, a characteristic of transformed epidermal cell lines (Díaz-Guerra, M., C. Bauluz, S. Haddow, J. L. Jorcano, A. Cano, A. Balmain, and M. Quintanilla, manuscript submitted for publication).

The possible involvement of P-cadherin, together with that of E-cadherin, in the final stage of epidermal carcinogenesis is presently being investigated by transfection of CarB cells with E- and/or P-cadherin cDNAs.

References

Aldaz, C. M., D. Trono, F. Larcher, T. J. Slaga, and C. J. Conti. 1989. Sequential trisomization of chromosomes 6 and 7 in mouse skin premalignant lesions. *Mol. Carcinogenesis.* 2:22–26.

Balmain, A., and K. Brown. 1988. Oncogene activation in chemical carcinogenesis. *Adv. Cancer Res.* 51:147–182.

Behrens, J., M. M. Mareel, F. M. VanRoy, and W. Birchmeier. 1989. Dissecting tumor cell invasion: epithelial cells acquire invasive properties after the loss of uvomorulin-mediated cell-cell adhesion. *J. Cell Biol.* 108:2435–2447.

Bianchi, A. B., C. M. Aldaz, and C. J. Conti. 1990. Nonrandom duplication of the chromosome bearing a mutated Ha-ras-1 allele in mouse skin tumors. *Proc. Natl. Acad. Sci. USA.* 87:6902–6906.

Boutwell, R. K. 1974. The function and mechanism of promoters of carcinogenesis. *CRC Crit. Rev. Toxicol.* 2:419–431.

Bremner, R., and A. Balmain. 1990. Genetic changes in skin tumor progression: correlation between presence of a mutant *ras* gene and loss of heterozygosity on mouse chromosome 7. *Cell.* 61:407–417.

Brown, K., M. Quintanilla, M. Ramsden, I. B. Kerr, S. Young, and A. Balmain. 1986. v-ras genes from Harvey and BALB murine sarcoma viruses can act as initiators of two-stage mouse skin carcinogenesis. *Cell.* 46:447–456.

Brown, K., A. Buchmann, and A. Balmain. 1990. Carcinogen-induced mutations in the mouse c-Ha-ras gene provide evidence of multiple pathways for tumor progression. *Proc. Natl. Acad. Sci. USA.* 87:538–542.

Chomczynski, P., and N. Sacchi. 1987. Single-step method of RNA isolation by acid guanidium thiocyanate-phenol-chloroform extraction. *Anal. Biochem.* 162:156–159.

Conti, C. J., C. M. Aldaz, J. O'Connell, A. J. Klein-Sanzto, and T. J. Slaga. 1986. Aneuploidy, an early event in mouse skin tumor development. *Carcinogenesis.* 7:1845–1848.

Edelman, G. M. 1985. Cell adhesion and the molecular processes of morphogenesis. *Annu. Rev. Biochem.* 54:135–169.

Eidelman, S., C. H. Damsky, M. J. Wheelock, and I. Damjanov. 1989. Expression of cell-cell adhesion glycoprotein cell-CAM 120/80 in normal human tissues and tumors. *Am. J. Pathol.* 15:101–110.

Eistetter, H. R., S. Adolph, M. Ringwald, D. Simon-Chazottes, R. Schuh, J. L. Guénet, and R. Kemler. 1988. Chromosomal mapping of the structural gene coding for the mouse cell adhesion molecule uvomorulin. *Proc. Natl. Acad. Sci. USA.* 85:3489–3493.

Feinberg, A. P., and B. Vogelstein. 1983. A technique for radiolabeling DNA restriction endonuclease fragments to high specific activity. *Anal. Biochem.* 132:6–13.

Frixen, U. H., J. Behrens, M. Sachs, G. Eberle, B. Voss, A. Warda, D. Löchner, and W. Birchmeir. 1991. E-cadherin-mediated cell-cell adhesion prevents invasiveness of human carcinoma cells. *J. Cell Biol.* 113:173–185.

Fusenig, N. E., D. Breitkreutz, R. T. Dzarlieva, P. Boukamp, E. Herzmann, A. Bohnert, J. Pöhlmann, C. Rausch, S. Schütz, and J. Hornung. 1982. Epidermal cell differentiation and malignant transformation in culture. *Cancer Forum.* 6:209–240.

Harber, D. A., A. J. Buckler, T. Glaser, K. M. Call, J. Pelletier, R. L. Sohn, E. C. Douglas, and D. E. Housman. 1990. An internal deletion within an 11p13 zinc finger gene contributes to the development of Wilm's tumor. *Cell.* 61:1257–1269.

Hashimoto, M., O. Niwa, Y. Nitta, M. Takeichi, and K. Yokoro. 1989. Unstable expression of E-cadherin adhesion molecules in metastatic ovarian tumor cells. *Jpn. J. Cancer Res.* 80:459–463.

Hatta, K., and M. Takeichi. 1986. Expression of N-cadherin adhesion molecule associated with early morphogenetic events in chick development. *Nature (Lond.).* 320:447–449.

Hatta, K., T. S. Okada, and M. Takeichi. 1985. A monoclonal antibody disrupting calcium-dependent cell-cell adhesion of brain tissues: possible role of its target antigen in animal pattern formation. *Proc. Natl. Acad. Sci. USA.* 82:2789–2793.

Hatta, K., A. Nose, A. Nagafuchi, and M. Takeichi. 1988. Cloning and expression of cDNA encoding a neural calcium-dependent cell adhesion molecule: its identity in the cadherin gene family. *J. Cell Biol.* 106:873–881.

Hecker, E. 1978. Structure-activity relationships in diterpene esters irritant and co-carcinogenic to mouse skin. *In* Carcinogenesis. Vol. 2. Mechanisms of Tumor Promotion and Co-carcinogenesis. T. J. Slaga, A. Sivak, and R. K. Boutwell, editors. Raven Press, New York. 11–48.

Henninngs, H., R. Shores, P. Mitchell, E. F. Spangler, and S. H. Yuspa. 1985. Induction of papillomas with a high probability of conversion to malignancy. *Carcinogenesis.* 6:1607–1610.

Hirano, S., A. Nose, K. Hatta, A. Kawakami, and M. Takeichi. 1987. Calcium-dependent cell-cell adhesion molecules (cadherins): subclass specificities and possible involvement of actin bundles. *J. Cell Biol.* 105:2501–2510.

Hyafil, F., D. Morello, C. Babinet, and F. Jacob. 1980. A cell surface glycoprotein involved in the compaction of embryonic carcinoma cells and cleavage stage embryos. *Cell.* 21:927–934.

Hynes, R. O. 1989. Oncogenic transformation. *In* Fibronectins. A. Rich, editor. Springer-Verlag, New York. 301–334.

Klein-Szanto, A. J. P., F. Larcher, R. D. Bonfil, and C. J. Conti. 1989. Multistage chemical carcinogenesis protocols produce spindle cell carcinomas of the mouse skin. *Carcinogenesis.* 10:2169–2172.

Koufos, A., P. Grundy, K. Morgan, K. A. Aleck, T. Hadro, B. C. Lampkin, A. Kalbakji, and W. K. Cavenee. 1989. Familial Wiedemann-Beckwith syndrome and a second Wilm's tumor locus map to 11p15.5. *Am. J. Hum. Genet.* 44:711–719.

Kulesz-Martin, M., A. E. Kilkenny, K. A. Holbrook, V. Digernes, and S. H. Yuspa. 1983. Properties of carcinogen altered mouse epidermal cells resistant to calcium induced terminal differentiation. *Carcinogenesis.* 4:1367–1377.

Laemmli, U. K. 1970. Cleavage of structural proteins during the assembly of the head of bacteriophage T4. *Nature (Lond.).* 227:680–685.

Maniatis, T., E. F. Fritsch, and J. Sambrook. 1982. Molecular cloning: a laboratory manual. Cold Spring Harbor Laboratory, Cold Spring Harbor, N.Y.

Miyatani, S., K. Shimamura, M. Hatta, A. Nagafuchi, A. Nose, M. Matsunaga, K. Hatta, and M. Takeichi. 1989. Neural cadherin: Role in selective cell-cell adhesion. *Science (Wash. DC).* 245:631–635.

Nagafuchi, A., and M. Takeichi. 1988. Cell binding function of E-cadherin is regulated by the cytoplasmic domain. *EMBO (Eur. Mol. Biol. Organ.) J.* 7:3679–3684.

Nagafuchi, A., Y. Shirayoshi, K. Okazaki, K. Yasuda, and M. Takeichi. 1987. Transformation of cell adhesion properties by exogenously introduced E-cadherin cDNA. *Nature (Lond.).* 329:341–343.

Nose, A., and M. Takeichi. 1986. A novel cadherin adhesion molecule: its expression patterns associated with implantation and organogenesis of mouse embryos. *J. Cell Biol.* 103:2649–2658.

Nose, A., A. Nagafuchi, and M. Takeichi. 1987. Isolation of placental cadherin cDNA: identification of a novel gene family for cell-cell adhesion molecules. *EMBO (Eur. Mol. Biol. Organ.) J.* 6:3655–3661.

Nose, A., A. Nagafuchi, and M. Takeichi. 1988. Expressed recombinant cadherins mediate cell sorting in model systems. *Cell.* 54:993–1001.

Parish, R. W., C. Schmidhauser, T. Schmidt, and R. Dudler. 1987. Mechanisms of tumour cell metastasis. *J. Cell Sci. Suppl.* 8:181–197.

Peyrieras, N., D. Louvard, and F. Jacob. 1985. Characterization of antigens recognized by monoclonal antibodies and polyclonal antibodies directed against uvomorulin. *Proc. Natl. Acad. Sci. USA.* 82:8067–8071.

Quintanilla, M., K. Brown, M. Ramsden, and A. Balmain. 1986. Carcinogen-specific mutation and amplification of Ha-ras during mouse skin carcinogenesis. *Nature (Lond.).* 322:78–80.

Quintanilla, M., S. Haddow, D. Jonas, D. Jaffe, G. T. Bowden, and A. Balmain. 1991. Comparison of *ras* activation during epidermal carcinogenesis in vitro and in vivo. *Carcinogenesis.* In press.

Rave, N., R. Crvenjacov, and H. Baedfker. 1979. Identification of procollagen mRNAs transferred to diazobenzylomethyl paper from formaldehyde agarose gels. *Nucleic Acids Res.* 11:3559–3567.

Ringwald, M., R. Schuh, D. Vestweber, H. Eistetter, F. Lottpeisch, J. Engel, R. Dolz, F. Jahnig, J. Epplen, S. Mayer, C. Muller, and R. Kemler. 1987. The structure of cell adhesion molecule uvomorulin. Insights into the molecular mechanism of Ca^{2+}-dependent adhesion. *EMBO (Eur. Mol. Biol. Organ.) J.* 6:3647–3653.

Shimoyama, Y., S. Hirohashi, S. Hirano, M. Noguchi, Y. Shimosato, M. Takeichi, and O. Abe. 1989. Cadherin cell-adhesion molecules in human epithelial tissues and carcinomas. *Cancer Res.* 49:2128–2133.

Shirayoshi, Y., T. S. Okada, and M. Takeichi. 1986. N-linked oligosaccharides are not involved in the function of a cell-cell binding glycoprotein E-cadherin. *Cell Struct. Funct.* 11:245–252.

Southern, P. J., and P. Berg. 1982. Transformation of mammalian cells to antibiotic resistance with a bacterial gene under the control of the SV40 early region promoter. *J. Mol. Appl. Genet.* 1:327–341.

Takeichi, M. 1988. The cadherins: cell-cell adhesion molecules controlling animal morphogenesis. *Development (Camb.).* 102:639–655.

Takeichi, M. 1990. Cadherins: a molecular family important in selective cell-cell adhesion. *Annu. Rev. Biochem.* 59:237–252.

Takeichi, M. 1991. Cadherin cell adhesion receptors as a morphogenetic regulator. *Science (Wash. DC).* 251:1451–1455.

Takeichi, M., C. Y. Noro, Y. Shirayoshi, and K. Hatta. 1985. Calcium-dependent cell adhesion system: its molecular nature, cell type specificity and morphogenetic role. *In* The Cell in Contact. G. M. Edelman and J. P. Thiery, editors. John Wiley & Sons, Inc., New York. 219–232.

Thiery, J. P., J. L. Duband, U. Rutishauser, and G. M. Edelman. 1982. Cell adhesion molecules in early chicken embryogenesis. *Proc. Natl. Acad. Sci. USA.* 79:6737–6741.

Towbin, H., T. Staehelin, and J. Gordon. 1979. Electrophoretic transfer of proteins from polyacrylamide gels to nitrocellulose sheets: procedure and some applications. *Proc. Natl. Acad. Sci. USA.* 82:4683–4687.

Yoshida-Noro, C., N. Suzuki, and M. Takeichi. 1984. Molecular nature of the calcium-dependent cell-cell adhesion system in mouse teratocarcinoma and embryonic cells studied with a monoclonal antibody. *Dev. Biol.* 101:19–27.